Acta Geophysica (2019) 67:799–811
https://doi.org/10.1007/s11600-019-00294-2

RESEARCH ARTICLE - APPLIED GEOPHYSICS

Frequency-dependent energy attenuation and velocity dispersion in periodic layered media

Heng Zhang[1] · Fanchang Zhang[1] · Yawei Lu[1]

Received: 15 November 2018 / Accepted: 22 April 2019 / Published online: 2 May 2019

Abstract
According to Brajanovski periodic layered model, a fractural medium can be equivalent to layered media with periodic distribution of fractural layers and background layers, but the analytical solution given by Brajanovski can only interpret the dispersion and attenuation effects of single characteristic unit model. In order to study the dispersion and attenuation features of multiple characteristic units, forward modeling methods are needed. Based on the theory of two-phase medium, Biot deduced the propagation equation of longitudinal waves in fluid-saturated porous media. However, there are two problems in the forward modeling using time-domain equation. One is the influences of boundary reflection, and the other is the introduction of cumulative error. For convenience, time-domain equation is rewritten in the frequency domain, thus constructing a one-dimensional rock physics model. Then, forward method is used to study the dispersion and attenuation features of fluid-saturated medium. Numerical simulation results are found to be in good agreement with the analytical solution. Furthermore, the frequency-domain forward method can analyze the velocity dispersion and energy attenuation of longitudinal waves in any multilayered fracture medium. By analyzing those numerical simulation results, it can be obtained that, as the length of characteristic unit increases or the number of characteristic unit decreases, both the starting frequency of dispersion and the peak frequency of attenuation shift to low, whatever the attenuation peaks are equal. In addition, the effects of porosity, permeability and fluid saturation on energy attenuation and velocity dispersion are also studied. Finally, the stress field and displacement field distributions of fluid-saturated fractural medium are given by the frequency-domain forward modeling method.

Keywords Attenuation · Dispersion · Fractural medium · Frequency-domain forward modeling

Introduction

In recent years, natural fractured reservoirs have attracted the interest of geophysicists in the fields of petroleum exploration and development. In many cases, natural fractures control the permeability of the reservoir, so the ability to find and characterize natural fracture areas of the reservoir is a major challenge for seismic exploration.

✉ Fanchang Zhang
zhangfch@upc.edu.cn

Heng Zhang
s17010186@s.upc.edu.cn

Yawei Lu
luyawei123456@gmail.com

[1] China University of Petroleum (East China), Qingdao, People's Republic of China

When discussing the seismic response of fluid-saturated porous media, the most commonly used theory is Biot's (1939, 1941, 1956a, b, 1962) two-phase medium theory, which divides fluid-saturated porous media into solid frame and porous fluids, respectively. Biot two-phase medium theory is the beginning of research on fluid-saturated porous media. The theory predicts the longitudinal wave velocity in fluid-saturated medium under the condition that the dry rock skeleton and fluid properties are known. The energy loss between the crest and trough of a longitudinal wave is called "Biot loss." However, the loss of fluid in the macroscopic background is much less than the loss in the seismic band (Pride et al. 2004). Mavko and Nur (1979) proposed a microscopic mechanism to explain the seismic wave attenuation of porous media. When seismic wave causes particle-scale background rupture, microcrack will generate larger fluid pressure than the pore space and then cause fluid to flow from microcrack into pore, called the "squirt flow." Dvorkin

et al. (1994) proposed a squirt flow model for fluid-saturated rocks and combined it with Biot theory to obtain Biot/squirt (BISQ) theory. Ba and Zhao (2016) developed a new dual-porosity medium based on squirt flow theory and proposed a new boundary to predict the longitudinal wave velocity of saturated dense rock. Although the squirt flow theory can fully explain and calculate the attenuation at ultrasonic frequencies, it fails to explain the attenuation produced in the seismic band. In recent years, Rubino et al. (2009) and Ba et al. (2012) have strongly proved that the most important reason for the dispersion and attenuation of longitudinal waves in the seismic frequency band is that the waves induced fluid flow (WIFF) in the mesoscopic scale. Dvorkin (2014) and Shen et al. (2018) study the mechanism for attenuation in the seismic frequency band and establish the relationship between velocity and formation absorption parameters.

The mechanism of attenuation and dispersion due to the presence of fluid in rock pore space is broadly called WIFF. Elastic wave creates pressure gradient in the fluid phase that causes the fluid to flow until fluid pressure reaches equilibrium under the action of internal friction. Because of the effect of WIFF, elastic parameters of the medium exhibit frequency-dependent features and then cause velocity dispersion and energy attenuation when elastic waves propagate in the subsurface medium, especially in oil and gas reservoirs. Gassmann–Biot theory (Gassmann 1951; Biot 1956a) gives the expression of the bulk modulus of fluid-saturated rock in an isotropic medium at low frequencies, and the theory becomes a very classic model for fluid replacement, but it only applied to isotropic media. For anisotropic background media with cracks, fractures, etc., Brown and Korringa (1975) derived an effective elastic modulus formula for anisotropic rock skeletons and fluid-saturated rocks. This model is equally applicable to low-frequency conditions and does not work well under laboratory ultrasonic conditions. White et al. (1975) first proposed a periodic layered patchy saturated model with the interlaced superposition of water and gas layers on the premise that the mesoscopic scale was attenuated by WIFF, and described the longitudinal wave dispersion and attenuation. Hudson et al. (1996) and Chapman (2003) developed a theoretical model of attenuation and dispersion due to wave-induced flow between cracks and pores; this model is developed for sparse penny-shaped cracks in porous matrices. Chapman (2002, 2003) proposed a medium model with aligned fractures under isotropic media conditions. Galvin and Gurevich (2003) and Brajanovski et al. (2005) calculated the stiffness matrix of porous media with aligned planar fractures and then calculated the attenuation and dispersion of fast longitudinal waves. Galvin and Gurevich (2009) proposed a complex pore space model composed of penny-shaped cracks and rigid pores and gave an expression for calculating the modulus of the model. A more general approach to modeling fractural porous media is based on Biot's theory of porous elasticity. In the context of Biot's theory, fractures can be thought of as heterogeneous formations with high compliance. Based on this assumption, a model of fractural medium can be constructed and then applied to study the wave propagation in non-uniform porous media.

In this paper, we only study the elastic wave response of a one-dimensional model. The characteristic units are stacked vertically with no horizontal heterogeneity. According to the Brajanovski periodic layered model, the fractural porous medium is equivalent to a layered medium in which the fracture layer and the background layer are periodically distributed. Combined with Gurevich et al. the periodically distributed fracture layer is regarded as a layer with high compliance and high porosity embedded in background porous medium, and an equivalent model of fractural porous medium is obtained. Then based on the Biot pore elasticity equation, we use the finite difference algorithm to carry out the forward modeling, to study the elastic characteristics of the porous media with plane fractures and to analyze the energy attenuation and velocity dispersion characteristics of the fast longitudinal waves. In addition, we examine the effects of three important parameters of porosity, permeability and fluid saturation on energy attenuation and velocity dispersion.

Elastic wave response with planar fracture medium

The main reason for the attenuation of elastic waves in fluid-saturated rocks is the WIFF. When elastic waves propagate in a fluid-saturated porous medium, a local pressure gradient is formed in the fluid phase, causing liquid flow and corresponding viscous friction until the pore pressure reaches equilibrium (Müller et al. 2010). When a simple harmonic wave propagates in a fluid-saturated porous medium, a part of the rock is compressed and the other part is expanded. High pore pressure is generated in the compression zone, and the pore fluid will flow from high pore pressure to low pressure, so that the relative flow of the fluid will cause energy loss. In other words, during the propagation of the wave, dispersion and attenuation occur due to the influence of WIFF.

According to the Brajanovski periodic layered model, the fractured porous medium can be equivalent to a layered medium with periodic distribution of the fracture layer and the background layer. Gurevich et al. assume that the fracture in the periodic layered medium is a thin layer with high compliance and high porosity. Thus, the fractural porous medium is equivalent to the model shown in Fig. 1 (White et al. 1975; Galvin and Gurevich 2003), where h represents the thickness of one characteristic unit, h_1 represents the thickness of the background porous medium, and h_2 represents the thickness

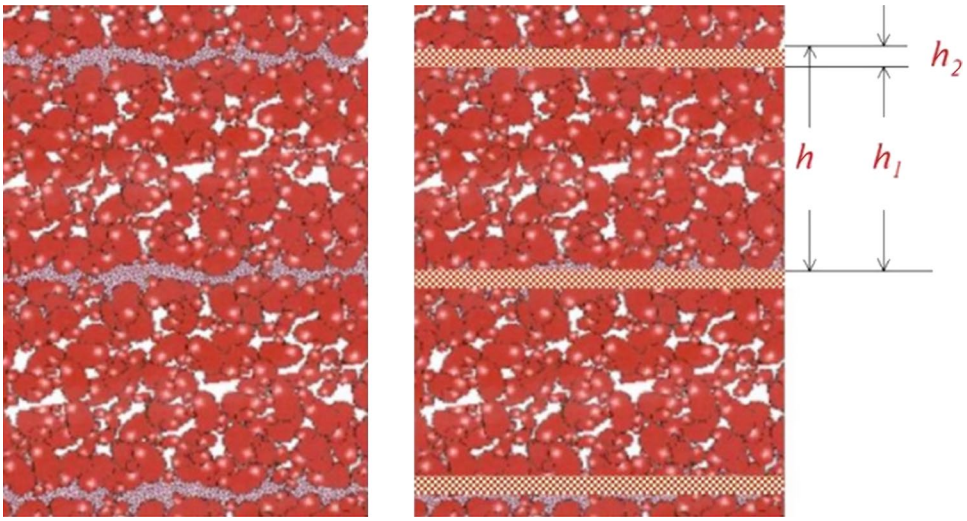

Fig. 1 Equivalent model of fractured porous media (Galvin and Gurevich 2003)

of the equivalent fracture layer; they are stacked together to form a single characteristic unit. The compressive forces cause fluid flow from the softer layer into the stiffer layer during wave propagation on the rock, which creates a pressure gradient between the layers and causes attenuation and dispersion. We will use this model to study the elastic wave response of fractural porous media at mesoscopic scale.

Assume that the symmetry axis of the medium is parallel to the *z*-axis; the layer is infinitely extended in the *xoy* plane. When the porous rock is dry or gas saturation, the stiffness matrix is as follows:

In Eq. (1), the brackets $\langle\cdot\rangle$ mean the thickness weighted average of the property, that is, $\langle q\rangle = q_c h_c + q_b h_b = (1-h_b)q_c + q_b h_b$, where h_b and h_c denote the thickness fraction of background layer and fracture layer, respectively. γ are the square of the shear wave velocity to the longitudinal wave velocity ration, $L = \lambda + 2\mu = K + 4\mu/3$ is the equivalent P-wave modulus, λ and μ are the Lame parameters, and K is bulk modulus.

Inversion of stiffness matrix $\mathbf{c}^{\mathrm{dry}}$ yields the compliance matrix $\mathbf{s}^{\mathrm{dry}} = (\mathbf{c}^{\mathrm{dry}})^{-1}$:

$$\mathbf{c}^{\mathrm{dry}} = \begin{bmatrix} \frac{(1-2\langle\gamma\rangle)^2}{\langle 1/L\rangle} + 4\langle\mu\rangle - 4\langle\gamma\mu\rangle & \frac{(1-2\langle\gamma\rangle)^2}{\langle 1/L\rangle} + 2\langle\mu\rangle - 4\langle\gamma\mu\rangle & \frac{1-2\langle\gamma\rangle}{\langle 1/L\rangle} & 0 & 0 & 0 \\ \frac{(1-2\langle\gamma\rangle)^2}{\langle 1/L\rangle} + 2\langle\mu\rangle - 4\langle\gamma\mu\rangle & \frac{(1-2\langle\gamma\rangle)^2}{\langle 1/L\rangle} + 4\langle\mu\rangle - 4\langle\gamma\mu\rangle & \frac{1-2\langle\gamma\rangle}{\langle 1/L\rangle} & 0 & 0 & 0 \\ \frac{1-2\langle\gamma\rangle}{\langle 1/L\rangle} & \frac{1-2\langle\gamma\rangle}{\langle 1/L\rangle} & \frac{1}{\langle 1/L\rangle} & 0 & 0 & 0 \\ 0 & 0 & 0 & \frac{1}{\langle 1/\mu\rangle} & 0 & 0 \\ 0 & 0 & 0 & 0 & \frac{1}{\langle 1/\mu\rangle} & 0 \\ 0 & 0 & 0 & 0 & 0 & \langle\mu\rangle \end{bmatrix} \tag{1}$$

$$\mathbf{s}^{\mathrm{dry}} = \begin{bmatrix} \frac{1-\langle\gamma\mu\rangle/\langle\mu\rangle}{3\langle\mu\rangle-4\langle\gamma\mu\rangle} & -\frac{1-2\langle\gamma\mu\rangle/\langle\mu\rangle}{2(3\langle\mu\rangle-4\langle\gamma\mu\rangle)} & -\frac{1-2\langle\gamma\rangle}{2(3\langle\mu\rangle-4\langle\gamma\mu\rangle)} & 0 & 0 & 0 \\ -\frac{1-2\langle\gamma\mu\rangle/\langle\mu\rangle}{2(3\langle\mu\rangle-4\langle\gamma\mu\rangle)} & \frac{1-\langle\gamma\mu\rangle/\langle\mu\rangle}{3\langle\mu\rangle-4\langle\gamma\mu\rangle} & -\frac{1-2\langle\gamma\rangle}{2(3\langle\mu\rangle-4\langle\gamma\mu\rangle)} & 0 & 0 & 0 \\ -\frac{1-2\langle\gamma\rangle}{2(3\langle\mu\rangle-4\langle\gamma\mu\rangle)} & -\frac{1-2\langle\gamma\rangle}{2(3\langle\mu\rangle-4\langle\gamma\mu\rangle)} & \left\langle\frac{1}{L}\right\rangle + \frac{(1-2\langle\gamma\rangle)^2}{3\langle\mu\rangle-4\langle\gamma\mu\rangle} & 0 & 0 & 0 \\ 0 & 0 & 0 & \left\langle\frac{1}{\mu}\right\rangle & 0 & 0 \\ 0 & 0 & 0 & 0 & \left\langle\frac{1}{\mu}\right\rangle & 0 \\ 0 & 0 & 0 & 0 & 0 & \frac{1}{\langle\mu\rangle} \end{bmatrix} \tag{2}$$

When the thickness of the fracture layer is infinite, that is, $h_c \to 0$, there is $\mu_c, L_c \to 0$, and $\langle \mu \rangle \to \mu_b$, $\langle \gamma \rangle \to \gamma_b$, $\left\langle \frac{1}{\mu} \right\rangle \to \frac{1}{\mu_b} + \lim_{h_c \to 0} \frac{h_c}{\mu_c}$, $\left\langle \frac{1}{L} \right\rangle \to \frac{1}{L_b} + \lim_{h_c \to 0} \frac{h_c}{L_c}$, $\langle \gamma \mu \rangle \to \gamma_b \mu_b$. μ_b and μ_c are the shear modulus of background and fracture layers, respectively. L_b and L_c are the P-wave modulus of background and fracture layers, respectively. Substitution of these results into Eq. (2) yields the compliance matrix of the dry fractured porous medium:

$$\begin{aligned} \mathbf{s}^{\mathrm{dry}} &= \mathbf{s}_{\mathrm{b}}^{\mathrm{dry}} + \mathbf{s}_{\mathrm{c}}^{\mathrm{dry}} \\ &= \begin{bmatrix} \frac{1}{E_b} & -\frac{\nu_b}{E_b} & -\frac{\nu_b}{E_b} & 0 & 0 & 0 \\ -\frac{\nu_b}{E_b} & \frac{1}{E_b} & -\frac{\nu_b}{E_b} & 0 & 0 & 0 \\ -\frac{\nu_b}{E_b} & -\frac{\nu_b}{E_b} & \frac{1}{E_b} & 0 & 0 & 0 \\ 0 & 0 & 0 & \frac{1}{\mu_b} & 0 & 0 \\ 0 & 0 & 0 & 0 & \frac{1}{\mu_b} & 0 \\ 0 & 0 & 0 & 0 & 0 & \frac{1}{\mu_b} \end{bmatrix} + \lim_{h_c \to 0} \begin{bmatrix} 0 & 0 & 0 & 0 & 0 & 0 \\ 0 & 0 & 0 & 0 & 0 & 0 \\ 0 & 0 & \frac{h_c}{L_c} & 0 & 0 & 0 \\ 0 & 0 & 0 & \frac{h_c}{\mu_c} & 0 & 0 \\ 0 & 0 & 0 & 0 & \frac{h_c}{\mu_c} & 0 \\ 0 & 0 & 0 & 0 & 0 & 0 \end{bmatrix} \end{aligned} \tag{3}$$

In Eq. (3) $E_b = \mu_b(3 - 4\gamma_b)/(1 - \gamma_b)$ denotes the dynamic Young's modulus of background porous layer and $\gamma_b = 1 - 2\gamma_b/[2(1 - \gamma_b)]$ denotes the dynamic Poisson's ratio of background porous layer. Matrices $\mathbf{s}_{\mathrm{b}}^{\mathrm{dry}}$ and $\mathbf{s}_{\mathrm{c}}^{\mathrm{dry}}$ are the compliance matrices caused by the dry background and dry fracture layers, respectively. Equation (3) is consistent with the equation for the compliance matrix of a fractural medium as given by linear slip deformation theory (Schoenberg and Douma 1988; Schoenberg and Sayers 2012).

Assuming the shear modulus μ_c and longitudinal modulus $K_c + 4\mu_c/3$ are

$\mathcal{O}(h_c)$ as $h_c \to 0$, and defining

$$\lim_{h_c \to 0} \frac{h_c}{L_c} = Z_{\mathrm{N}}, \lim_{h_c \to 0} \frac{h_c}{\mu_c} = Z_{\mathrm{T}}, \tag{4}$$

where Z_{N} and Z_{T} are called excess normal and tangential compliances, respectively, Fang et al. (2013) demonstrate the relations between Z_{N}, Z_{T} and fractures infill material properties. These results also verify the correct rationality of the assumption that the fracture layer is a thin layer with high compliance and high porosity.

However, when the pore space is saturated with fluid, the rock exhibits frequency-dependent velocity dispersion and attenuation due to the effect of WIFF between pores and fractures. Elastic waves in such a periodically layered and porous medium with periodic and segmental constant coefficients can be described by the Biot's equation of poroelasticity (Biot 1962).

The fluid-saturated P-wave modulus of layer is given by Gassmann's equation

$$C = L + \alpha^2 M \tag{5}$$

In Eq. (5), $\alpha = 1 - K_{\mathrm{dry}}/K_{\mathrm{g}}$ denotes Biot–Wills parameter and $1/M = (\alpha - \phi)/K_{\mathrm{g}} + \phi/K_{\mathrm{f}}$ denotes the bulk modulus of pore space.

White et al. (1975) and Norris (1993) showed that for frequencies much smaller than the Biot's characteristic frequency $\omega_{\mathrm{B}} = \eta\phi/\kappa\rho_{\mathrm{f}}$ and also much smaller than the resonant frequency of the layering $\omega_{\mathrm{R}} = V_{\mathrm{p}}/H$, the P-wave modulus c_{33}^{sat} of a periodic lamellar porous medium composed of alternating fracture layers and background layers in fluid saturation can be expressed as:

$$\frac{1}{c_{33}^{\mathrm{sat}}} = \left\langle \frac{1}{C} \right\rangle + \frac{2}{\sqrt{i\omega\eta}H} \frac{\left(\frac{\alpha_b M_b}{C_b} - \frac{\alpha_c M_c}{C_c} \right)^2}{\sqrt{\frac{M_b L_b}{C_b \kappa_b}} \cot\left(\sqrt{\frac{i\omega\eta C_b}{\kappa_b M_b L_b}} \frac{h_b H}{2} \right) + \sqrt{\frac{M_c L_c}{C_c \kappa_c}} \cot\left(\sqrt{\frac{i\omega\eta C_c}{\kappa_c M_c L_c}} \frac{h_c H}{2} \right)} \tag{6}$$

In Eq. (6) ω is circular frequency, η is the viscosity of the pore fluid.

H denotes the thickness of a characteristic unit, and h_b and h_c are the thickness fraction of background layer and fracture layer, respectively. κ_b and κ_c are the permeability of the background layer and fracture layer, respectively. Subscript b indicates the elastic parameters of the background layer, and subscript c indicates the elastic parameters of fracture layer.

After obtaining the equivalent longitudinal wave modulus of the fluid-saturated medium in the vertical direction, the velocity dispersion and energy attenuation perpendicular to the layered medium can be obtained by the following Eq. (7).

$$\begin{aligned} V_{\mathrm{p}} &= \sqrt{c_{33}^{\mathrm{sat}}/\rho} \\ 1/Q &= \mathrm{Im}(c_{33}^{\mathrm{sat}})/\mathrm{Re}(c_{33}^{\mathrm{sat}}) \end{aligned} \tag{7}$$

In Eq. (7) $\rho = h_b[\phi_b\rho_f + (1 - \phi_b)\rho_g] + h_c[\phi_c\rho_f + (1 - \phi_c)\rho_g]$ denotes the density of the rock. ρ_b and ρ_c are the density of the background and fracture layers, respectively. ϕ_b and ϕ_c are the porosity of the background and fracture layers, respectively.

One-dimensional frequency-domain forward method

The analytical solution given in the previous section can only describe the attenuation and dispersion features of a single characteristic unit. In order to study the seismic response of multiple characteristic units, we will use the numerical simulation method of finite difference forward modeling based on Biot theory. Under the assumption of

linear elasticity and isotropic medium, Biot gives the equation that P-waves satisfy in fluid-saturated porous media:

$$\begin{aligned} &-\nabla\cdot\sigma+\alpha\nabla p=f\\ &\frac{\partial}{\partial t}\left(\frac{p}{M}+\alpha\nabla\cdot\mathbf{u}\right)-\nabla\cdot\frac{\kappa}{\eta}\nabla p=g \end{aligned} \tag{8}$$

where f and g are the body forces and fluid forces acting on the porous medium, respectively. σ is stress, p is fluid pressure, $\mathbf{u}$ are solid displacement matrix; α is Biot–Wills coefficient, M is the bulk modulus of pore space, κ is permeability, and η is fluid viscosity.

To simplify the research, we just consider a P-wave propagating in the z-direction, assuming that the body forces and fluid forces are vanishing, Eq. (8) can be simplified as:

$$\begin{aligned} &-(\lambda+2\mu)\frac{\partial^2 u}{\partial z^2}+\alpha\frac{\partial p}{\partial z}=0\\ &\frac{\partial}{\partial t}\left(\frac{p}{M}+\alpha\frac{\partial u}{\partial z}\right)-\frac{\kappa}{\eta}\frac{\partial^2 p}{\partial z^2}=0 \end{aligned} \tag{9}$$

where λ and μ are the Lame parameters. In order to perform the forward modeling, the differential processing of the above formula is as follows:

$$\begin{aligned} &-\frac{U_{i-1}^{t+1}-2U_i^{t+1}+U_{i+1}^{t+1}}{\Delta z^2}+\frac{P_i^{t+1}-P_{i-1}^{t+1}}{\Delta z}=0\\ &\frac{1}{\Delta t}\left(\frac{P_{i+1}^{t+1}}{M}-\frac{P_i^t}{M}+\frac{U_{i+1}^{t+1}-U_i^{t+1}}{\Delta z}-\frac{U_{i+1}^{t+1}-U_i^{t+1}}{\Delta z}\right)\\ &=\frac{1}{2}\frac{\kappa}{\eta}\left(\frac{P_{i-1}^{t+1}-2P_i^{t+1}+P_{i+1}^{t+1}}{\Delta z^2}+\frac{P_{i-1}^{t}-2P_i^{t}+P_{i+1}^{t}}{\Delta z^2}\right) \end{aligned} \tag{10}$$

where U is the solid-phase displacement, P is the fluid pressure, superscript indicates different nodes, and subscripts indicate different moments. Δt is time step, and Δz is space grid step size. In order to ensure the stability of the differential forward, it is required that within a time step Δt, the wavelength does not pass more than one grid step Δz (Yang et al. 2003).

Equation (10) can be used to calculate the fluid pressure and solid displacement field distribution at any time when the wave propagates in a two-phase medium. If we want to obtain the velocity dispersion and attenuation of the medium, the absorbing boundary condition needs to be added. However, the forward modeling in the time domain needs to consider whether the boundary reflection is completely absorbed, and it is also possible that the iterative operation produces a large cumulative error, which has a great influence on the result. So we consider using the frequency-domain forward modeling method to study the elastic wave response in two-phase media.

Under the assumption that the stress divergence of the porous medium is zero, the one-dimensional form of the quasi-static Biot equation of linear consolidation coupling in the frequency-space domain is:

$$\begin{aligned} &\frac{\partial\tau_{zz}}{\partial z}=0\\ &\tau_{zz}=\left(K_{\mathrm{dry}}+\frac{4}{3}\mu_{\mathrm{dry}}\right)\frac{\partial U_{\mathrm{s}}}{\partial z}-\alpha P\\ &\frac{\partial U_{\mathrm{f}}}{\partial z}+\alpha\frac{\partial U_{\mathrm{s}}}{\partial z}+\frac{P}{M}=0\\ &j\omega U_{\mathrm{f}}+\frac{\kappa}{\eta}\frac{\partial P}{\partial z}=0 \end{aligned} \tag{11}$$

where τ_{zz} is the strain of the solid frame, P is the fluid pressure, U_{s} is the displacement of the solid, U_{f} is the displacement of fluid relative to solid, and K_{dry} and μ_{dry} are the bulk modulus and shear modulus of the solid frame, respectively. α is Biot–Wills parameter, M is the bulk modulus of pore space, ω is circular frequency, κ is permeability, and η is the viscosity of pore fluid.

Using the Taylor series expansion to expand Eq. (11) into the frequency-domain difference format, we obtain the following:

$$\begin{aligned} &\frac{\tau_{zz}(i+1)-\tau_{zz}(i-1)}{2\mathrm{d}z}=0\\ &\tau_{zz}(i)=\left(K_{\mathrm{dry}}+\frac{4}{3}\mu_{\mathrm{dry}}\right)\frac{U_{\mathrm{s}}(i+1)-U_{\mathrm{s}}(i-1)}{2\mathrm{d}z}-\alpha P(i)\\ &\frac{U_{\mathrm{f}}(i+1)-U_{\mathrm{f}}(i-1)}{2\mathrm{d}z}+\alpha\frac{U_{\mathrm{s}}(i+1)-U_{\mathrm{s}}(i-1)}{2\mathrm{d}z}+\frac{P(i)}{M}=0\\ &j\omega U_{\mathrm{f}}(i)+\frac{\kappa}{\eta}\frac{P(i+1)-P(i-1)}{2\mathrm{d}z}=0 \end{aligned} \tag{12}$$

where i is the ith grid point.

When numerical simulation is performed using Eq. (12), it is necessary to apply an external force at the upper and lower interfaces to simulate the role of simple harmonics wave. In addition, in order to ensure the closed condition of the petrophysical model, the fluid displacement of the upper and lower boundaries is zero. So the boundary conditions are:

$$\begin{aligned} &\tau_{zz}^{\mathrm{upper}}=\tau_{zz}^{\mathrm{lower}}=p_0\\ &U_{\mathrm{f}}^{\mathrm{upper}}=U_{\mathrm{f}}^{\mathrm{lower}}=0 \end{aligned} \tag{13}$$

where $\tau_{zz}^{\mathrm{upper}}$ and $\tau_{zz}^{\mathrm{lower}}$ are the stress of the upper interface and lower interface, respectively. $U_{\mathrm{f}}^{\mathrm{upper}}$ and $U_{\mathrm{f}}^{\mathrm{lower}}$ are the relative displacement of fluid at the upper and lower interfaces (Wu and Wu 2018), respectively.

Using the frequency-domain difference format Eq. (12), combined with the boundary condition Eq. (13), the finite

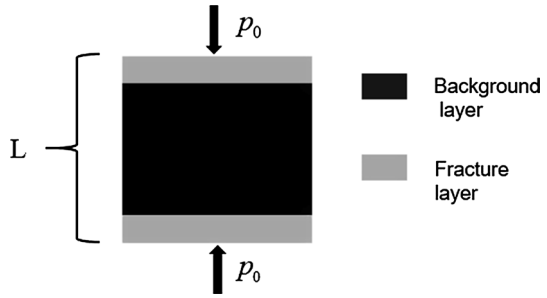

Fig. 2 Sketch of the model

difference numerical simulation method can be used to obtain the solid displacement value U_s at any point in the model medium. In the case of a known solid displacement field distribution, the overall strain of the model medium can be determined to satisfy:

$$e = \frac{U_s^{\text{lower}} - U_s^{\text{upper}}}{L} \tag{14}$$

where U_s^{upper} and U_s^{lower} are the solid displacement of the upper interface and lower interface, respectively.

When the medium is subjected to an external force p_0, the medium generates a bulk strain e, their ratio is the equivalent plane wave modulus E of the medium.

$$E = \frac{p_0}{e} \tag{15}$$

Because of the effect of WIFF, the modulus is frequency dependent, $E(\omega)$, and then velocity dispersion and energy attenuation satisfy:

$$\begin{aligned} V_P(\omega) &= \sqrt{\text{Re}[E(\omega)]/\rho} \\ Q^{-1}(\omega) &= \text{Im}[E(\omega)]/\text{Re}[E(\omega)] \end{aligned} \tag{16}$$

where Re( ) and Im( ) are the real and imaginary parts of the plural, respectively.

ρ is the density satisfying:

$$\rho = h_b[\rho_g \cdot (1-\phi_b) + \rho_f \cdot \phi_b] + h_c[\rho_g \cdot (1-\phi_c) + \rho_f \cdot \phi_c] \tag{17}$$

where h_b, ρ_b and ϕ_b are the thickness fraction, density and porosity of the background layer, respectively. h_c, ρ_c and ϕ_c are the thickness fraction, density and porosity of the fracture layer, respectively.

Numerical simulation

It is assumed that the fluid-saturated horizontal layered is periodically arranged alternately, and the lateral is infinitely extended. In order to study the elastic wave response of layered porous media with planar fractures, firstly, we compare the agreement between the white analytical solution and the frequency-domain forward modeling to verify the correctness and rationality of frequency-domain forward modeling, and then we change the parameters such as the number of

Table 1 Porous media parameter

Skeleton parameter	Fluid parameter	Fracture layer parameter	Background layer parameter
$K_g = 33.4$ Gpa	$K_f = 2.2$ Gpa	$K_{dry} = 0.6$ Gpa	$K_{dry} = 6$ Gpa
$\mu_g = 22$ Gpa	$\rho_f = 1000\,\text{kg/m}^3$	$\mu_{dry} = 0.3$ Gpa	$\mu_{dry} = 5$ Gpa
$\rho_g = 2650\,\text{kg/m}^3$	$\eta = 1\times10^{-3}$ pa s	$\phi_c = 0.8$	$\phi_b = 0.2$
		$k_c = 5\times10^{-10}\,\text{m}^2$	$k_b = 3\times10^{-13}\,\text{m}^2$

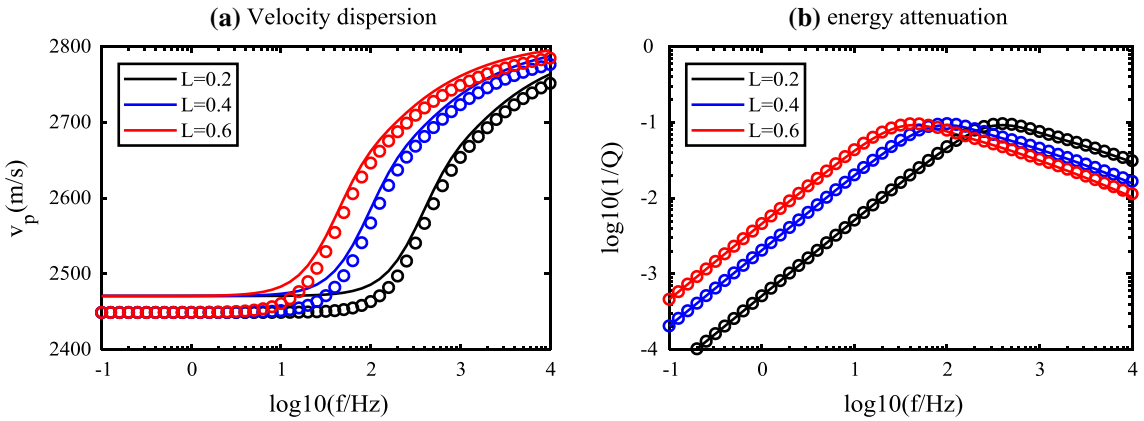

Fig. 3 P-wave velocity dispersion (**a**) and energy attenuation (**b**)

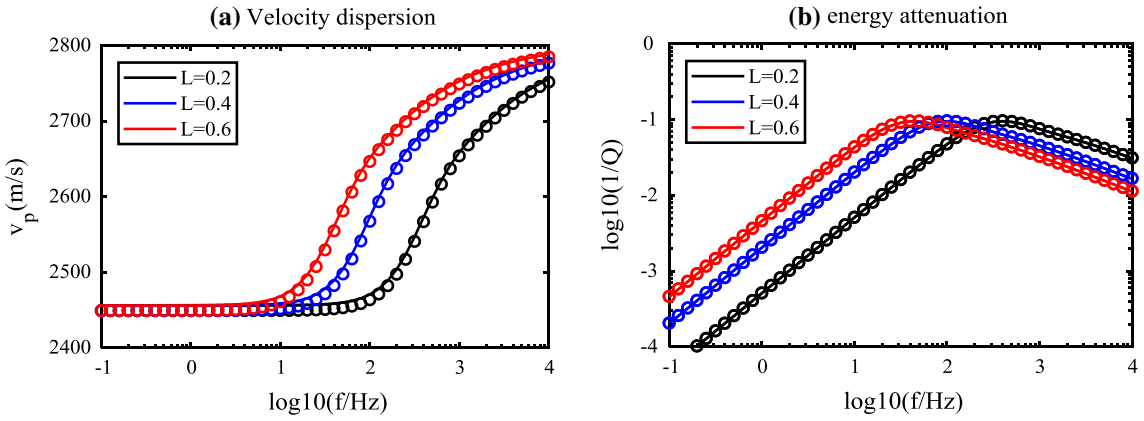

Fig. 4 P-wave velocity dispersion (**a**) and energy attenuation (**b**)

characteristic units, fracture thickness, fluid saturation, background porosity and permeability, to analyze the variation of the elastic wave response and compare with the previous research results to confirm the correctness of the research results (Galvin and Gurevich 2003; Brajanovski et al. 2005; Galvin and Gurevich 2009; Wu and Wu 2018).

Suppose the model contains only one characteristic unit and the thickness of the fracture layer is 0.1L; the sketch of the model is shown in Fig. 2. In Fig. 2, p_0 is an external force applied to the upper and lower interfaces. From top to bottom, there are fracture layer with thickness of 0.05L, background layer with thickness of 0.9L, and fracture layer with thickness of 0.05L; these three parts form a single characteristic unit.

Correctness, accuracy and computational efficiency of frequency-domain forward modeling

Firstly, we will verify the correctness of the frequency-domain forward method. Depending on the model in Fig. 2 and pore medium parameters in Table 1, the velocity dispersion and energy attenuation of Brajanovski layered medium with planar fractures are studied by analytical solution expression and frequency-domain numerical simulation. Their results are shown in Figs. 3 and 4.

Figure 3 and 4 shows the P-wave velocity dispersion and energy attenuation, the solid line represents the Brajanovski analytical solution, and the dotted line denotes the result of numerical simulation. The black curve, the blue curve and the red curve correspond to the characteristic unit thicknesses of 0.2 m, 0.4 m and 0.6 m, respectively. In Fig. 3, the model is divided into 400 grid points in the vertical direction for numerical simulation, and we can see the results of numerical simulation are in poor agreement with the analytical solution, especially in the low-frequency region. We deduce the reason for this error may be because the grid step size is too large. So we split the model into 900 grid points and the obtained results are shown in Fig. 4; the numerical simulation results are consistent with the analytical solution results. By comparing Fig. 3 with Fig. 4, we can conclude that when the grid points are small, it may cause the forward to produce dispersion phenomenon. Appropriately

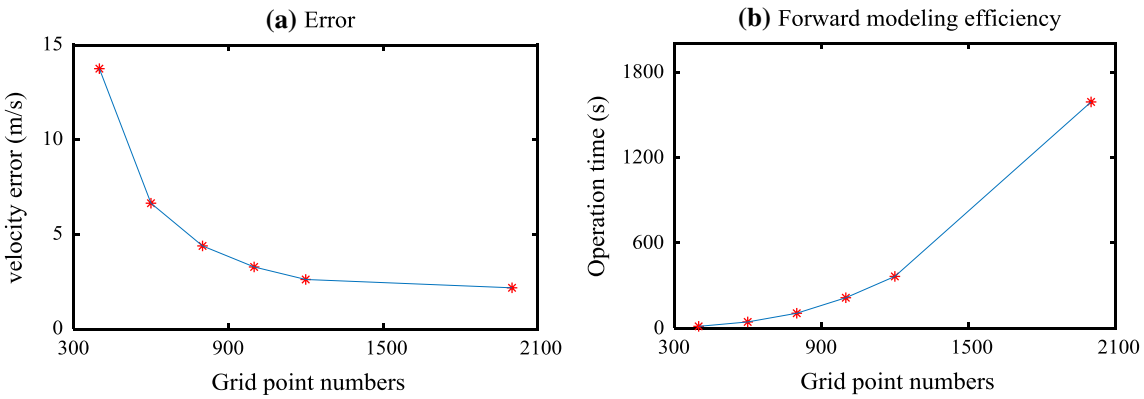

Fig. 5 Calculation accuracy (**a**) and efficiency (**b**) of finite difference forward modeling

increasing the number of gridding points can effectively weaken the dispersion phenomenon and reduce the error between the numerical simulation results and the analytical solution.

The relationship between accuracy and efficiency of differential forward modeling and the number of grid points is analyzed. Assuming that the model length is 0.2 m and contains only one characteristic unit, the model parameters used in the numerical simulation are shown in Table 1. The result is presented in Fig. 5.

It can be observed in Fig. 5 that, as the number of grid points increases, the error between numerical simulation and analytical solution decreases rapidly. When the number of grid points is greater than 800, the longitudinal wave velocity error is not more than 5 m/s. When the number of grid points is further increased, the velocity error does not decrease significantly, and the time spent on numerical simulation increases rapidly. In summary, we believe that when the number of grid points is between 800 and 1000, the calculation accuracy and efficiency can be satisfied. So in later studies, the model was divided into 800 grid points in the vertical direction.

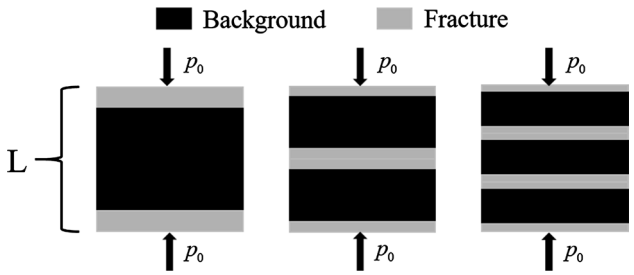

Fig. 6 Media model with different characteristic units

Influence of the length and number of characteristic units and thickness of fracture layer on elastic wave response

Firstly, we analyze the velocity dispersion and energy attenuation corresponding to different lengths of the characteristic unit. From the left of Fig. 4, we can see that as the length of the characteristic unit increases, the starting frequency of the velocity dispersion decreases, but the velocity corresponding to the low-frequency limit and the high-frequency limit does not vary. As can be seen on the right of Fig. 4, the attenuation peak remains unchanged, but the peak frequency shifts toward low frequency as the length of the characteristic unit increases.

Then, we analyze velocity dispersion and energy attenuation corresponding to multiple characteristic units. Assume that the total thickness of the medium is constant, divided it into different numbers of characteristic units, and the fracture thickness fraction in each characteristic unit is 10%. The model media with different numbers of characteristic units are forwarded separately to study the attenuation and dispersion features of the porous media with planar fractures.

As shown in Fig. 6, the model is divided into one, two and three characteristic units for forward modeling, and the corresponding elastic wave response is shown in Fig. 7. It can be seen from Fig. 7a that as the number of characteristic unit increases, the low-frequency limit velocity does not change, but the high-frequency limit velocity decreases, and the dispersion start frequency shifts to high-frequency direction. In Fig. 7b, the energy attenuation peaks have the same magnitude, but the frequency corresponding to the attenuation peak shifts toward high-frequency direction as the number of characteristic unit increases. This is because as the number of characteristic unit increases, the thickness of the single characteristic unit and the thickness of the fracture

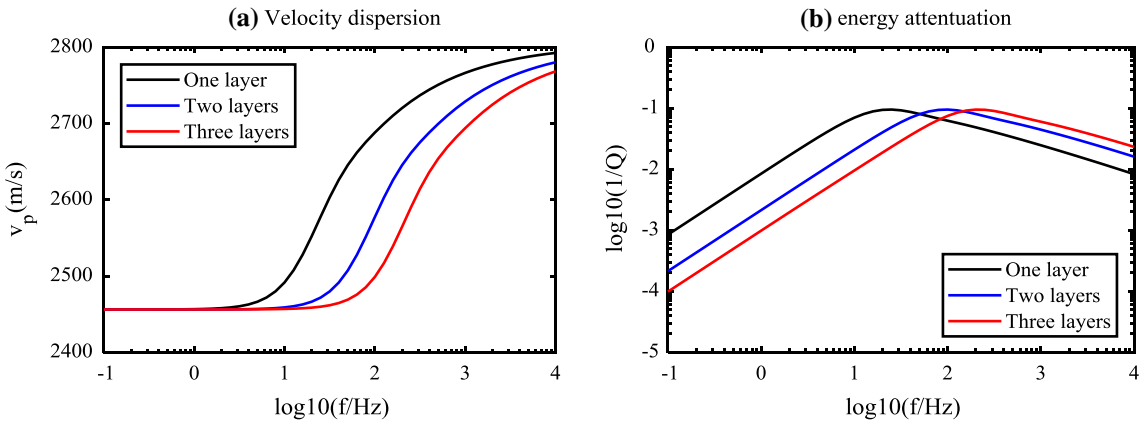

Fig. 7 Velocity dispersion (**a**) and attenuation (**b**) corresponding to the number of different feature units

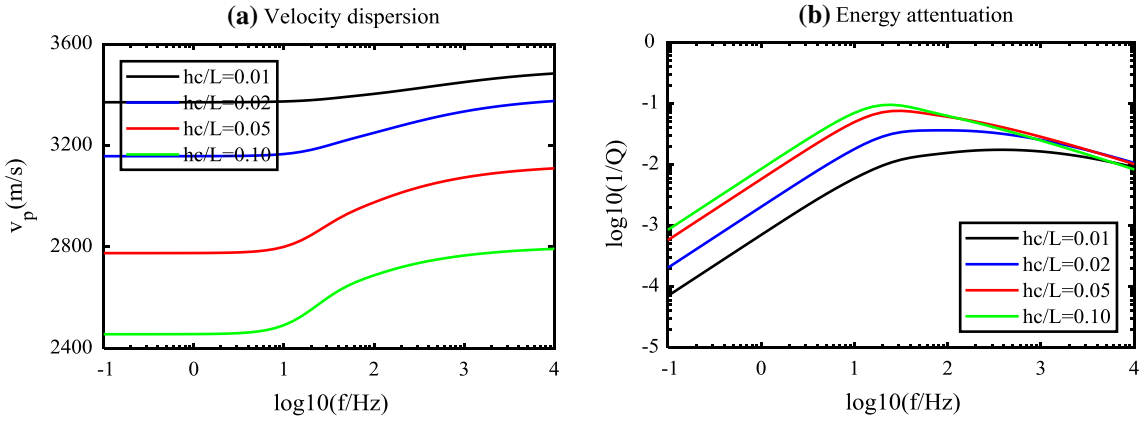

Fig. 8 Velocity dispersion (**a**) and attenuation (**b**) for different crack thicknesses

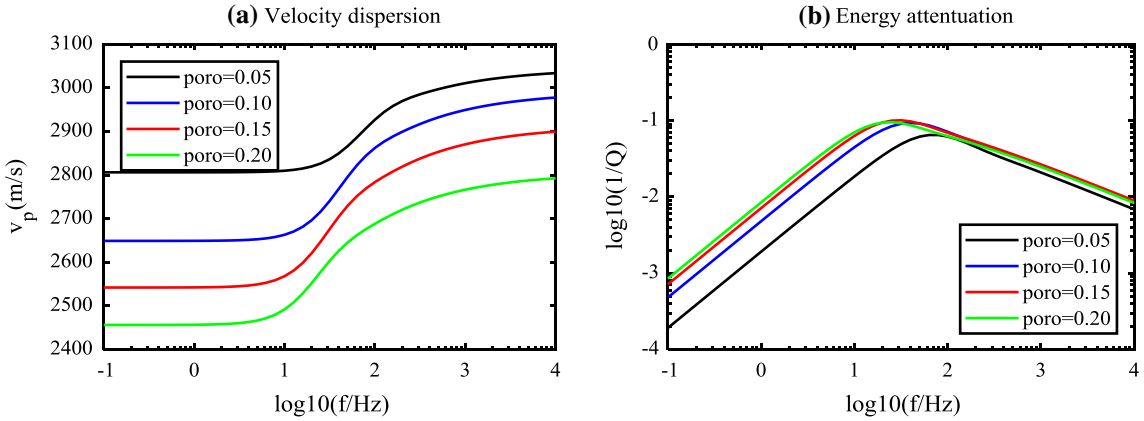

Fig. 9 Velocity dispersion (**a**) and attenuation (**b**) of porosity in different background layers

layer decrease, causing the initial frequency of the velocity dispersion and energy attenuation to move to high frequency.

Further study is carried out when the thickness of the medium $L = 0.4$ m remains unchanged, the variation features of velocity dispersion and energy attenuation when the thickness of fracture layer is changed. Assuming that the media contains only one characteristic unit, the thickness of fracture layer accounts for 0.01, 0.02, 0.05 and 0.1 of the total thickness of the medium, respectively. The forward result is shown in Fig. 8. It can be seen from the curve shown in Fig. 8a that as the thickness of fracture layer increases, the medium velocity decreases overall and the velocity dispersion is more severe in the seismic band. In Fig. 8b, the attenuation peak becomes larger and the peak frequency shifts toward low frequency. The reason for the velocity decrease is that the compliance of the medium increases due to the increase in the soft layer volume fraction, and the equivalent plane wave modulus of the medium decreases. At the same time, the increase in the fracture layer thickness leads to an increase in the overall porosity of the medium, so that the relative flow of the fluid is more likely to occur, thereby generating a stronger energy attenuation.

Influence of porosity, permeability and gas saturation on elastic wave response

Keep the porosity of fracture layer unchanged, and study the attenuation and dispersion features of porous medium when the porosity of the background layer changes. Assuming that the medium is a single feature unit, background layer porosity is 0.05, 0.10, 0.15 and 0.20, respectively. It can be observed in Fig. 9 that as the porosity of background layer increases, the wave velocity decreases as a whole, and the dispersion degree first increases and then slowly decreases. Attenuation peak increases first and then decreases, and the peak frequency gradually shifts to low frequency. At low frequencies, the fluid pressure of the medium can reach equilibrium in half a wave period, but it cannot reach equilibrium at high frequencies. However, as the porosity of background layer increases, the difficulty of the internal pressure of the

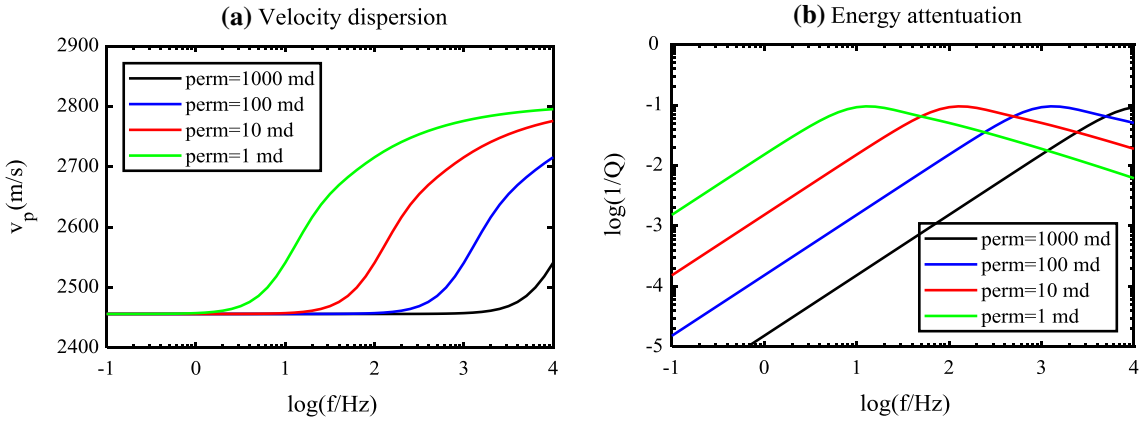

Fig. 10 Velocity dispersion (**a**) and attenuation (**b**) at different background layer permeabilities

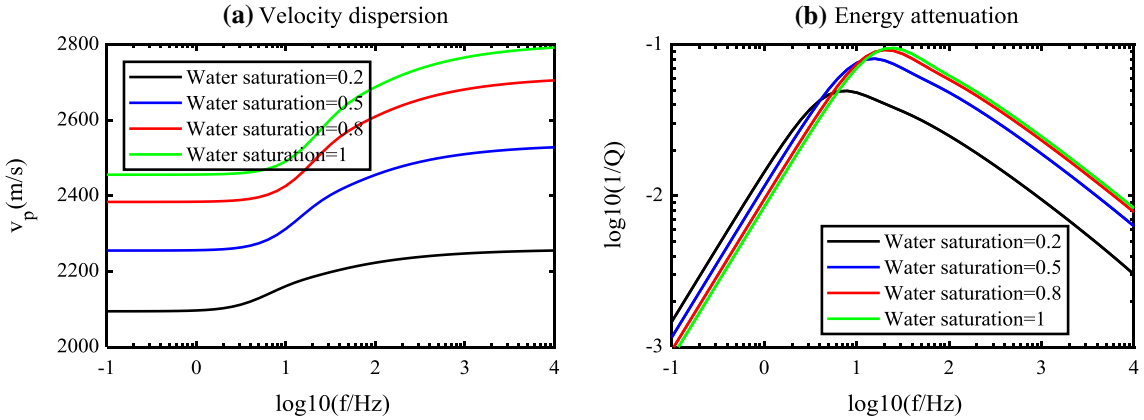

Fig. 11 Velocity dispersion (**a**) and attenuation (**b**) for different fluid saturations

medium reaching equilibrium is gradually reduced. Especially at high frequencies, due to the increase in porosity, the fluid still has a certain flow capacity at high frequencies, which reduces the high-frequency limit of bulk modulus, resulting in a decrease in the high-frequency velocity, causing the energy attenuation to increase first and then slowly decrease.

The effect of changing background layer permeability on the velocity dispersion and energy attenuation is studied when the fracture layer permeability remains ($k_c = 5 \times 10^{-10}$ m^2) unchanged. Assuming that the medium contains one characteristic unit, the permeability of background layer is 1×10^{-12} m^2, 1×10^{-13} m^2, 1×10^{-14} m^2 and 1×10^{-15} m^2, respectively. It can be seen from the curve shown in Fig. 10 that as the permeability of the background layer increases, the low-frequency velocity of the medium remains substantially unchanged, the high-frequency velocity decreases, and the initial frequency of the velocity dispersion shifts toward high-frequency direction. Energy attenuation peak remains substantially unchanged, and the peak frequency shifts to high frequency. We can deduce that the greater the difference in permeability between the background layer and the fracture layer, the lower the starting frequency of velocity dispersion and the peak frequency of energy attenuation.

We also study the elastic wave response when the fluid saturation in porous medium is different, assuming that the pores are filled with two fluids, gas and water. The saturation of water is s_a, the saturation of the gas is s_b, and $s_a + s_b = 1$ is established. The water saturation used for the forward performance is 0.2, 0.5, 0.8 and 1.0, respectively. It can be seen from Fig. 11 that as the water saturation increases, the velocity of the low-frequency limit and high-frequency limit increases, but the shape of the velocity dispersion curve is basically maintained constant. The energy attenuation peak is slightly increased, and the corresponding peak frequency shifts slightly to high-frequency direction, which is consistent with the conclusions obtained by the predecessors (Masson and Pride 2010; Zhang and He 2015). We believe that this phenomenon is caused by an increase in water saturation, which increases the equivalent P-wave modulus, resulting in an increase in velocity. And the increase in water saturation

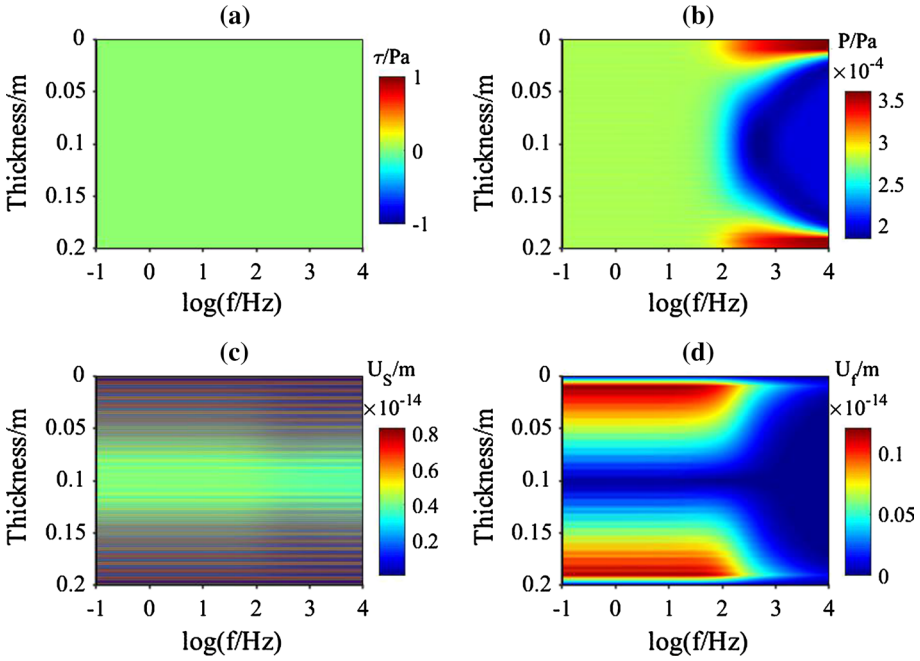

Fig. 12 Force field and displacement field distribution in a model under constant pressure: (**a**) the stress on the solid skeleton, (**b**) the force of the pore fluid, (**c**) the displacement of the solid skeleton under the external force and (**d**) the fluid displacement under pressure

means a decrease in gas saturation. Since water is more difficult to compress than gas, when the water saturation increases, the resistance of the elastic wave propagating in the medium also increases, resulting in an increase in the attenuation peak.

In addition, we can use forward modeling to simulate the force field and displacement field distribution in layered media. Assume that the model length is 0.2 m, the model extends wirelessly in the horizontal direction, which contains only one characteristic unit, the proportion of fracture layer is 10% of the total thickness, and elastic parameters of the medium are shown in Table 1. The model is divided into 800 grid points in the vertical direction for numerical simulation, and a constant force is applied to the upper and lower interfaces of the model. The distribution of the force field and the displacement field inside the model can be obtained as shown in Fig. 12.

It can be seen from Fig. 12a that the solid stress is uniform and independent of frequency, satisfying the assumption that the stress divergence of the porous medium is zero as previously mentioned. And in Fig. 12b the fluid pressure in the fracture layer and background layer is about 2.7×10^{-4} pa at low frequencies, but the fluid pressure in the fracture layer increases at high frequencies, while the fluid pressure in the background pores is reduced. In Fig. 12c, the solid displacement is sensitive to the combination of characteristic unit, because the fracture has high compliance and is easy to be compressed, so the solid-phase displacement of the fracture layer is large, while the displacement of the background porous medium is small. In Fig. 12d, the fluid displacements at the upper and lower boundaries of the model are zero, and near the fracture layer are obviously larger than the background layer at low frequencies, but at high frequencies the fluid displacement is zero. The reason for fluid pressure and fluid displacement is frequency dependent is that fluid movement is hindered at high frequencies, resulting in fracture layer is subjected to more external forces as a highly compliant layer.

It is worth mentioning that the model used in all numerical simulations is that the fracture layer is distributed at the top and bottom, and the external force acts directly on it. When we change the combination of the characteristic units, the fracture layer is embedded in the background porous medium. At this time, the top and bottom of the model is the background porous medium, and then loading stresses at the boundaries of the model to study the elastic wave response. From the results of velocity dispersion and energy attenuation of different characteristic units, under the same fracture volume fraction, the elastic wave energy attenuation and velocity dispersion curves of the characteristic unit models with different combinations are also different. However, it is worth noting that the high- and low-frequency limits of different feature unit velocities are consistent and that the energy attenuation is on the order of magnitude. At the same time, the curve change features caused by the change of elastic parameters are consistent. The corresponding figure is not included for brevity.

Discussion

The numerical simulation method in this paper can obtain high-precision results for the frequency-domain seismic wave attenuation and dispersion of the one-dimensional

model, but the theory is not applicable when the model is transverse anisotropy or even more complex. From the results of numerical simulation, we can infer that when the fluid-saturated reservoir contains a certain amount of gas, the seismic wave attenuation is relatively large, indicating the potential value of using the seismic wave attenuation for oil and gas prediction. In addition, the attenuation coefficient of the low-frequency band is linear with the frequency in the logarithmic coordinate system and thus can be used as a constraint condition for the inversion coefficient parameter Q. And it can qualitatively explain the high-frequency dispersion and high attenuation in the actual rock of the seismic frequency band.

Conclusion

The dispersion property of periodically layered medium with planar fracture is characterized by the finite difference forward method in frequency domain. By increasing the number of differential meshes, the natural dispersion of differential algorithm can be effectively weakened, and the frequency-domain forward results agreed with the Brajanovski analytical solution, which verified the correctness of frequency-domain differential forward method. It provides an accurate and reasonable method for studying the elastic wave response of Brajanovski layered media with planar fractures.

The dispersion and attenuation of fluid-saturated medium with different porosities, permeabilities and fluid saturations are analyzed. The results show that the thicker the fractural layer, the more easily the velocity dispersion occurs, and the larger the attenuation peak, the lower the peak frequency. As the porosity increases, the frequency of dispersion shifts to low frequency, the attenuation peak increases first and then decreases, and the peak frequency gradually moves to the low-frequency direction. As the permeability increases, the high-frequency velocity decreases slightly, the starting frequency of dispersion moves toward high-frequency direction, and the peak of attenuation is nearly the same, while the peak frequency moves to the high-frequency direction. As the water saturation increases, the velocity increases as a whole, the degree of dispersion increases, the peak of energy attenuation increases, and the peak frequency increases slightly.

For the horizontally layered medium with high-angle fracture, the corresponding dispersion and attenuation properties such as HTI media need to be further studied.

Acknowledgements We are grateful to the reviewers for their constructive comments on this paper. This research is supported by the following funds: the National Natural Science Foundation of China (Nos. 41874146 and 41874149).

Compliance with ethical standards

Conflict of interest On behalf of all authors, the corresponding author states that there is no conflict of interest.

References

Ba J, Carcione JM, Cao H et al (2012) Velocity dispersion and attenuation of P waves in partially-saturated rocks: wave propagation equations in double-porosity medium. Chin J Geophys 55(1):219–231. https://doi.org/10.6038/j.issn.0001-5733.2012.01.021

Ba J, Zhao J, Carcione JM et al (2016) Compressional wave dispersion due to rock matrix stiffening by clay squirt flow. Geophys Res Lett 43(12):6186–6195. https://doi.org/10.1002/2016GL069312

Biot MA (1939) Non-linear theory of elasticity and the linearized case for a body under initial stress. Philos Mag 27(183):468–489. https://doi.org/10.1080/14786443908562246

Biot MA (1941) General theory of three-dimensional consolidation. J Appl Phys 12(2):155–164. https://doi.org/10.1063/1.1712886

Biot MA (1956a) Theory of propagation of elastic waves in a fluid-saturated porous solid. I. Low-frequency range. J Acoust Soc Ame 28(2):168–178. https://doi.org/10.1121/1.1908239

Biot MA (1956b) Theory of propagation of elastic waves in a fluid-saturated porous solid. II. Higher frequency range. J Acoust Soc Am 28(2):179–191. https://doi.org/10.1121/1.1908241

Biot MA (1962) Mechanics of deformation and acoustic propagation in porous media. J Appl Phys 33(4):1482–1498. https://doi.org/10.1063/1.1728759

Brajanovski M, Gurevich B, Schoenberg M (2005) A model for P-wave attenuation and dispersion in a porous medium permeated by aligned fractures. Geophys J R Astron Soc 163(1):372–384. https://doi.org/10.1111/j.1365-246X.2005.02722.x

Brown RJS, Korringa J (1975) On the dependence of the elastic properties of a porous rock on the compressibility of the pore fluid. Geophysics 40(4):608–616. https://doi.org/10.1190/1.1440551

Chapman M (2003) Frequency dependent anisotropy due to meso-scale fractures in the presence of equant porosity. Geophys Prospect 51(5):369–379. https://doi.org/10.1046/j.1365-2478.2003.00384.x

Chapman M, Zatsepin SV, Crampin S (2002) Derivation of a microstructural poroelastic model. Geophys J R Astron Soc 151(2):427–451. https://doi.org/10.1046/j.1365-246X.2002.01769.x

Dvorkin J, Nolenhoeksema RC, Nur A (1994) The squirt-flow mechanism: macro-scopic description. Geophysics 59(3):428–438. https://doi.org/10.1190/1.1443605

Dvorkin J, Gutierrez MA, Grana D (2014) Seismic reflections of rock properties. Cambridge University Press, Cambridge. https://doi.org/10.1017/cbo9780511843655

Fang X, Shang X, Fehler M (2013) Sensitivity of time-lapse seismic data to fracture compliance in hydraulic fracturing. Geophys J Int 195(3):1843–1861. https://doi.org/10.1190/segam2013-0732.1

Galvin RJ, Gurevich B (2003) Frequency-dependent anisotropy of porous rocks with aligned fractures. In: ASEG 16th geophysical conference and exhibition, Adelaide. https://doi.org/10.1111/1365-2478.12177

Galvin RJ, Gurevich B (2009) Effective properties of a poroelastic medium containing a distribution of aligned cracks. J Geophys Res Solid Earth 114(1):1–11. https://doi.org/10.1029/2008JB006032

Gassmann F (1951) Über die Elastizität Poröser Medien: Vierteljschrift.der naturforschenden. Gesellschaft in zürich 96:1–23

Hudson JA, Liu E, Crampin S (1996) The mechanical properties of materials with interconnected cracks and pores. Geophys J R

Astron Soc 124(1):105–112. https://doi.org/10.1111/j.1365-246X.1996.tb06355.x

Masson YJ, Pride SR (2010) Finite-difference modeling of Biot's poroelastic equations across all frequencies. Geophysics 75(2):33–41. https://doi.org/10.1190/1.3332589

Mavko GM, Nur A (1979) Wave attenuation in partially saturated rocks. Geophysics 44(2):161–178. https://doi.org/10.1190/1.440958

Müller TM, Gurevich B, Lebedev M (2010) Seismic wave attenuation and dispersion resulting from wave-induced flow in porous rocks—a review. Geophysics 75(5):147–164. https://doi.org/10.1190/1.3463417

Norris AN (1993) Low-frequency dispersion and attenuation in partially saturated rocks. J Acoust Soc Am 94(1):359–370. https://doi.org/10.1121/1.407101

Pride SR, Berryman JG, Harris JM (2004) Seismic attenuation due to wave-induced flow. J Geophys Res 109(1):1–19. https://doi.org/10.1029/2003JB002639

Rubino JG, Ravazzoli CL, Santos JE (2009) Equivalent viscoelastic solids for heterogeneous fluid-saturated porous rocks. Geophysics 74(1):1–13. https://doi.org/10.1190/1.3008544

Schoenberg M, Douma J (1988) Elastic-wave propagation in media with parallel fractures and aligned cracks. Geophys Prospect 36(6):571–590. https://doi.org/10.1111/j.1365-2478.1988.tb.2181.x

Schoenberg M, Sayers CM (2012) Seismic anisotropy of fractured rock. Geophysics 60(1):204–211. https://doi.org/10.1190/1.1443748

Shen Y, Dvorkin J, Li Y (2018) Improving seismic Qp estimation using rock physics constraints. Geophysics 83(3):1–56. https://doi.org/10.1190/geo2016-0655.1

White JE, Mihailova N, Lyakhovitsky F (1975) Low-frequency seismic waves in fluid-saturated layered rocks. J Acoust Soc Am J 11(10):654–659. https://doi.org/10.1121/1.1995164

Wu J, Wu G (2018) Quantitative virtual rock physics method in one-dimensional frequency domain. Pet Geophys Prospect 53(1):105–112. https://doi.org/10.13810/j.cnki.issn.1000-7210.2018.01.013

Yang J, Song E, Chen Z (2003) Analysis of two compression waves of saturated soil by finite difference method of u-w equation. Chin J Appl Mech 20(4):89–92. https://doi.org/10.3969/j.issn.1000-4939.2003.04.020

Zhang H, He B (2015) Propagation and attenuation of P-waves in patchy saturated porous media. Appl Geophys 12(3):401–408. https://doi.org/10.1007/s11770-015-0497-x